2 × 2 Superstructure in Sodium Cobalt Oxide Superconductors

ARTICLE *in* CHEMISTRY OF MATERIALS · AUGUST 2009

Impact Factor: 8.35 · DOI: 10.1021/cm8031237

8 AUTHORS, INCLUDING:

Kazunori Takada
National Institute for Materials Science
245 PUBLICATIONS **7,079** CITATIONS
SEE PROFILE

Yong Nam Choi
Korea Atomic Energy Research Institute (KA…
59 PUBLICATIONS **455** CITATIONS
SEE PROFILE

Dimitri N. Argyriou
European Spallation Source
233 PUBLICATIONS **5,770** CITATIONS
SEE PROFILE

Hiroya Sakurai
National Institute for Materials Science
139 PUBLICATIONS **2,271** CITATIONS
SEE PROFILE

CHEMISTRY OF MATERIALS
Article

Chem. Mater. **2009,** *21,* 3693–3700 3693
DOI:10.1021/cm8031237

2×2 Superstructure in Sodium Cobalt Oxide Superconductors

Kazunori Takada,*[,†,⊥] Mitsuko Onoda,[†,⊥] Yong-Nam Choi,[‡] Dimitri N. Argyriou,[§] Fujio Izumi,[†] Hiroya Sakurai,[†] Eiji Takayama-Muromachi,[†] and Takayoshi Sasaki[†,⊥]

[†]*National Institute for Materials Science, 1-1 Namiki, Tsukuba, Ibaraki 305-0044, Japan,* [‡]*Korea Atomic Energy Research Institute, 150 Deokjin-dong, Yuseong-gu, Daejeon 305-353, Korea,* [§]*Hahn-Meitner-Institut, Glienicker Strasse 100, Berlin D-14109, Germany, and* [⊥]*Japan Science and Technology Agency, 4-1-8, Honcho, Kawaguchi, Saitama 332-0012, Japan*

Received November 17, 2008. Revised Manuscript Received June 26, 2009

Crystal structures of sodium cobalt oxide bilayer-hydrates were analyzed on the basis of superstructure models by assuming that the host and guest layers are commensurate. The superstructure model gave better fitting results compared to the incommensurate composite crystal model, suggesting that the host and guest layers are commensurate and have a 2×2 superstructure. Although the Co−O bonds in the superconductive CoO_2 layers were reported to be shorter than that was expected from the Co oxidation states, the bond lengths refined in this study were consistent with the oxidation states.

Introduction

Sodium cobalt oxide bilayer-hydrates[1] are very unique not only in terms of their superconductivity but also crystal structures. Unusual structural features were suggested by diffuse bands observed in their neutron diffraction (ND) patterns;[2] however, they had not been disclosed until our previous study.[3]

Two kinds of hydrates showing superconductivity have been synthesized: one derived from γ-$Na_{0.7}CoO_2$,[1a] the other from α-$NaCoO_2$.[1b,1c] The CoO_2 layers in the former are stacked with two-layer periodicity to form a double hexagonal structure (2H phase), whereas those in the latter are stacked with three-layer periodicity, resulting in a rhombohedral unit cell (3R phase). The first unique feature is that the arrangement of guests including Na^+ ions and H_2O molecules between the CoO_2 host layers is common to the two phases in spite of the different stacking manner of the CoO_2 layers. That is, the two phases have the same guest structure in spite of the different host structures.

The guest arrangement itself is also very unique. The guests are ordered in the galleries between the host layers to form a $2/\sqrt{3}a \times 2/\sqrt{3}a$ trigonal lattice (intralayer ordering), where a is an in-plane lattice constant of the host lattice. On the other hand, along the c-direction, when a guest layer is stacked onto another over the interposed CoO_2 layer, the stacking is accompanied by a lateral shift with shift vectors, $1/2\boldsymbol{a}_2$, $1/2\boldsymbol{a}_2 + 1/2\boldsymbol{b}_2$, and $1/2\boldsymbol{b}_2$, where $\boldsymbol{a}_2$ and $\boldsymbol{b}_2$ are lattice vectors of the $2/\sqrt{3}a \times 2/\sqrt{3}a$ lattice, with the same probability (interlayer short-range ordering).[4]

Although our previous study had already revealed this basic crystal structure,[3] further structure refinement has become important. The remarkable structural feature that differentiates the superconductors from their nonsuperconducting counterparts is the large interlayer distance of 9.8 Å. Therefore, the high two-dimensionality induced by the large separation between CoO_2 layers is considered to play an important role in the superconductivity, which is strongly supported by the disappearance of superconductivity in partially dehydrated monolayer phases along with shrinkage of the interlayer distance to 6.9 Å.[5] On the other hand, a recently proposed phase diagram[6] suggests that the structure of the CoO_2 layer itself is also important, because the bilayer hydrates are sometimes nonsuperconducting in spite of their interlayer distance of 9.8 Å.[6,7] The relationship between the structure of the CoO_2 layer and the electronic properties has

*To whom correspondence should be addressed. E-mail: takada.kazunori@nims.go.jp.

(1) (a) Takada, K.; Sakurai, H.; Takayama-Muromachi, E.; Izumi, F.; Dilanian, R. A.; Sasaki, T. *Nature* **2003**, *422*, 53. (b) Takada, K.; Sakurai, H.; Takayama-Muromachi, E.; Izumi, F.; Dilanian, R. A.; Sasaki, T. *Adv. Mater.* **2004**, *16*, 1901. (c) Foo, M. L.; Klimczuk, T.; Li, L.; Ong, N. P.; Cava, R. J. *Solid State Commun.* **2005**, *133*, 407.
(2) (a) Lynn, J. W.; Huang, Q.; Brown, C. M.; Miller, V. L.; Foo, M. L.; Schaak, R. E.; Jones, C. Y.; Mackey, E. A.; Cava, R. J. *Phys. Rev.* **2003**, *B68*, 214516. (b) Jorgensen, J. D.; Avdeev, M.; Hinks, D. G.; Burley, J. C.; Short, S. *Phys. Rev.* **2003**, *B68*, 214517. (c) Argyriou, D. N.; Radaelli, P. G.; Milne, C. J.; Aliouane, A.; Chapon, L. C.; Chemseddine, A.; Veira, J.; Cox, S.; Mathur, N. D.; Midgley, P. A. *J. Phys.: Condens. Matter* **2005**, *17*, 3293.
(3) Takada, K.; Onoda, M.; Argyriou, D. N.; Choi, Y. −N.; Izumi, F.; Sakurai, H.; Takayama-Muromachi, E.; Sasaki, T. *Chem. Mater.* **2007**, *19*, 3519.
(4) Onoda, M.; Takada, K.; Argyriou, D.; Choi, Y. −N.; Sasaki, T. *Philos. Mag.* **2007**, *87*, 2773.
(5) (a) Foo, M. L.; Schaak, R. E.; Miler, V. L.; Klimczuk, T.; Rogado, N. S.; Wang, Y.; Lau, G. C.; Craley, C.; Zandbergen, H. W.; Ong, N. P.; Cava, R. J. *Solid State Commun.* **2003**, *127*, 33. (b) Takada, K.; Sakurai, H.; Takayama-Muromachi, E.; Izumi, F.; Dilanian, R. A.; Sasaki, T. *J. Solid State Chem.* **2004**, *177*, 372. (c) Takada, K.; Osada, M.; Izumi, F.; Sakurai, H.; Takayama-Muromachi, E.; Sasaki, T. *Chem. Mater.* **2005**, *17*, 2034.
(6) (a) Sakurai, H.; Takada, K.; Sasaki, T.; Takayama-Muromachi, E. *J. Phys. Soc. Jpn.* **2005**, *74*, 2909. (b) Sakurai, H.; Tsujii, N.; Suzuki, O.; Kitazawa, H.; Kido, G.; Takada, K.; Sasaki, T.; Takayama-Muromachi, E. *Phys. Rev.* **2006**, *B74*, 092502.
(7) Mistry, S.; Arnold, D. C.; Nuttall, C. J.; Lappas, A.; Green, M. A. *Chem. Commun.* **2004**, 2440.

Published on Web 07/17/2009

been experimentally[8] and theoretically[9] investigated. More precise details on the structure of the CoO_2 layer are necessary in order to verify the second scenario.

In our previous structural study, the hosts and guests were arranged in $a\times a$ and $2/\sqrt{3}a\times 2/\sqrt{3}a$ trigonal lattices, respectively, and the latter was unfolded into a $2a\times 2a$ lattice in the final refinement. Although the structural analysis was based on the assumption that they were incommensurate, the lattice constant of $2/\sqrt{3}a$ suggests that the host and guest layers are commensurate with each other and unfolded into a common $2a\times 2a$ lattice.[4] If this is true, structural analysis based on the commensurate model will reveal structural modulation in the CoO_2 layers forming the $2a\times 2a$ superlattice, which may be important for elucidating the superconducting mechanism. In the present study, the crystal structures were analyzed based on commensurate models in order to get such information on the superconductors.

Experimental Section

The powder ND data reported in ref 3 were used in this study. Details of the sample preparation and diffraction measurement and the chemical compositions determined by chemical analyses were also presented in the report.

The crystal structures were analyzed based on composite crystal models,[10] in which the structures were separated into host and guest systems, and the diffraction patterns were simulated by matrix method.[11] In the matrix method, the stacking manner was expressed by a probability table, in which the probabilities denoted by p(layer-1, layer-2) that the ith and $(i+1)$th layers are layer-1 and layer-2 are tabularized. A computer program, FU1,[12] was used to calculate the diffraction intensities, which were converted into that for the corresponding powder samples by another program, PPROF and summed up into powder patterns by PSIM.[13] The simulated patterns were fitted to the observed ones by least-squares method.

Crystal structures were visualized, and bond valence sums were calculated by VICS.[14]

Results

Brief Description of the Previous Analysis Using an Incommensurate Model. In the previous structure analysis, the guest layers are assumed to be incommensurate with the host layers. Because the present structure analysis using a commensurate model was based on the results of the previous analysis, a brief description is in order.

Structure models of the host and guest layers used in the previous analysis are shown in Figure 1, in which lattice

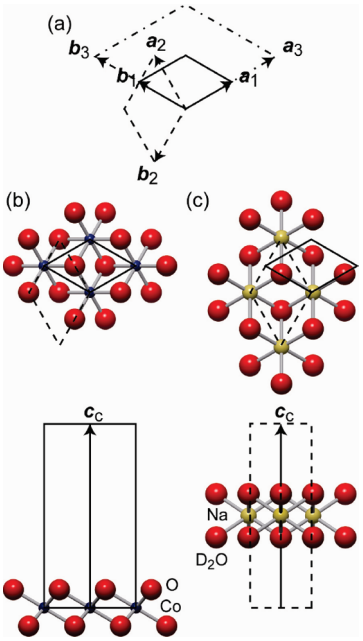

Figure 1. (a) Relationship between in-plane lattice vectors in $a\times a$, $2/\sqrt{3}a\times 2/\sqrt{3}a$, and $2a\times 2a$ trigonal lattices; and basic crystal structure of (b) host and (c) guest layers.

vectors for the structure models were set as $\boldsymbol{a}_1 \equiv \boldsymbol{a}_{2H} = \boldsymbol{a}_{3R}$, $\boldsymbol{b}_1 \equiv \boldsymbol{b}_{2H} = \boldsymbol{b}_{3R}$, and $\boldsymbol{c}_c \equiv 1/2\boldsymbol{c}_{2H} = 1/3\boldsymbol{c}_{3R}$, where $\boldsymbol{a}_{2H}$, $\boldsymbol{b}_{2H}$, and $\boldsymbol{c}_{2H}$ are lattice vectors for the host subsystem in the 2H phase, while $\boldsymbol{a}_{3R}$, $\boldsymbol{b}_{3R}$, and $\boldsymbol{c}_{3R}$ are those in the 3R phase. The lattice vectors for the $2/\sqrt{3}a\times 2/\sqrt{3}a$ guest lattice, $\boldsymbol{a}_2$ and $\boldsymbol{b}_2$, are defined as $2/3\boldsymbol{a}_1 + 4/3\boldsymbol{b}_1$ and $-4/3\boldsymbol{a}_1 - 2/3\boldsymbol{b}_1$, respectively, as shown in Figure 1a.

When $H_{1'}$ is generated from H_1 in Figure 1b by a symmetry operation of $(x, y, -z)$, the stacking to form the double hexagonal structure of the host subsystem in the 2H phase can be expressed as $p(H_r, H_{r'}) = 1$ for $r \neq r'$, and $p(H_r, H_{r'}) = 0$ for $r = r'$. On the other hand, the stacking to form the rhombohedral lattice in the 3R phase can be expressed as $p(H_1, H_2) = p(H_2, H_3) = p(H_3, H_1) = 1$, otherwise $p(H_r, H_{r'}) = 0$, where H_2 and H_3 are generated from H_1 by shift vectors of $2/3\boldsymbol{a}_1 + 1/3\boldsymbol{b}_1$ and $1/3\boldsymbol{a}_1 + 2/3\boldsymbol{b}_1$, respectively.

Contrary to the regular stacking, or long-range ordering, in the host subsystems, the guest layers are stacked with the "interlayer short-range ordering". The guest subsystem is composed of four kinds of guest layers, G_1, G_2, G_3, and G_4, which are generated from G1 in Figure 1c by lateral shifts of $\boldsymbol{0}$, $1/2\boldsymbol{a}_2$, $1/2\boldsymbol{a}_2 + 1/2\boldsymbol{b}_2$, and $1/2\boldsymbol{b}_2$, respectively. Probabilities for the guest stacking are $p(G_p, G_{p'}) = 0$ for $p = p'$, and $p(G_p, G_{p'}) = 1/3$ for $p \neq p'$.

Commensurate Model for the 2H Phase and Structure Refinement. The objective of this study is finding out whether the host and guest layers are commensurate and refining the $2a\times 2a$ superstructures, if they are commensurate. It may sound strange that we cannot conclude the commensuration yet, although the $a\times a$ host and $2/\sqrt{3}a\times 2/\sqrt{3}a$ guest lattices can be unfolded into a common $2a\times 2a$ lattice. It should be mentioned that the same lattice constants alone do not mean the commensurate relation between the host and guest subsystems. For example,

(8) Ihara, Y.; Ishida, K.; Michioka, C.; Kato, M.; Yoshimura, K.; Takada, K.; Sasaki, T.; Sakurai, H.; Takayama-Muromachi, E. *J. Phys. Soc. Jpn.* **2005**, *74*, 867.
(9) (a) Mochizuki, M.; Ogata, M. *J. Phys. Soc. Jpn.* **2006**, *75*, 113703. (b) Mochizuki, M.; Ogata, M. *J. Phys. Soc. Jpn.* **2007**, *76*, 013704.
(10) Janner, A.; Janssen, T. *Acta Crystallogr., Sect. A* **1980**, *A36*, 408.
(11) (a) Hendricks, S.; Teller, E. *J. Chem. Phys.* **1942**, *10*, 147. (b) Kakinoki, J.; Komura, Y. *Acta Crystallogr.* **1965**, *19*, 137. (b) Kakinoki, J. *Acta Crystallogr.* **1967**, *23*, 875.
(12) (a) Kato, K.; Kosuda, K.; Koga, T.; Nagasawa, H. *Acta Crystallogr., Sect. C* **1990**, *46*, 1587.(b) Kato, K. FU1, personal communication, **1991**.
(13) Kato, K. PPROF and PSIM, personal communication, **1998**.
(14) Izumi, F.; Dilanian, R. A. *CPD-IUCr Newslett.* **2005**, *32*, 59.

even when the host and guest lattices are refined to have the same lattice constants, there may be small differences of the lattice constants beyond the significant digits. Even such a slight difference makes the subsystems incommensurate as explained in the Supporting Information. Therefore, we have to analyze the structure based on a commensurate model and compare the result with that from the incommensurate model in order to leach the conclusion on the commensuration.

In addition, structural modulation was neglected in the previous study. In the composite crystal, interaction between the subsystems causes modulation in the structures including fractional coordinates, occupancies, atomic displacement parameters, etc. To take the modulation into account, a high-dimensional formalism should be used as in superspace group theory. However, the guest subsystem show the "interlayer short-range stacking" to give the diffuse pattern. Because there are no established calculation approaches based on high-dimensional formalisms for the disordered structure, the contribution of the modulation was assumed to be small enough to be neglected in our previous study. On the other hand, the modulation can be taken into account without using a high-dimensional formalism, when the subsystems are commensurate. When the host and guest layers are unfolded into a common superlattice, it is possible to make the structure modulation included in structure parameters themselves, because some atoms on special positions in a fundamental structure model are rearranged into more general positions with more refinable parameters. Therefore, we used the following superstructure model to express commensurate relation in this study.

To construct the superstructure model, the hosts and guests must be arranged in a common $2a \times 2a$ trigonal lattice, and their alternate stacking must be expressed in one probability table. When the $2/\sqrt{3}a \times 2/\sqrt{3}a$ guest lattice is unfolded into a $2a \times 2a$ lattice as shown in Figure 1a, the four kinds of guest layers in the former should be unfolded into twelve in the latter as indicated in Table 1. Guest structure based on this model was already refined in ref 3, and the $a \times a$ host lattice can be simply unfolded into the $2a \times 2a$ lattice. They were used in the superstructure model with the following modification.

In the incommensurate model, the hosts and guests were arranged in $a \times a \times c_c$ and $2/\sqrt{3}a \times 2/\sqrt{3}a \times c_c$ lattices, which were respectively piled up to host and guest subsystems. Co and Na atoms were set on $z = 0$ and $z = 1/2$ planes in the host and guest lattices, respectively, in order to interpenetrate the subsystems. On the other hand, the host and guest lattices should be stacked alternately in the commensurate model. Therefore, both host and guest lattices should have dimensions of $2a \times 2a \times 1/2c_c$, in which Co and Na are on the $z = 0$ plane.

The host and guest layers are alternately stacked to form the layered structure. Therefore, the layered structure can be expressed as stacked guest − host pairs, $G_{pq}-H_r$, formed by stacking a host layer onto a guest layer. Since H_1 and $H_{1'}$ are alternately stacked in the 2H phase, $p(G_{pq}-H_r, G_{p'q'}-H_{r'}) = 0$ for $r = r'$. In addition, the "interlayer short-range ordering" requires that $p(G_{pq}-H_r, G_{p'q'}-H_{r'}) = 0$ for $p = p'$. The probability table meeting these requirements was constructed as follows.

Table 1. Guest Layers in the $2/\sqrt{3}a \times 2/\sqrt{3}a$ Lattice and Shift Vectors for Generating Guest Layers in the $2a \times 2a$ Lattice

guest layer	shift vector	guest layer	shift vector
G_1	$\boldsymbol{0}$	G_{11}	$\boldsymbol{0}$
		G_{12}	$2/3\boldsymbol{a}_3 + 1/3\boldsymbol{b}_3$
		G_{13}	$1/3\boldsymbol{a}_3 + 2/3\boldsymbol{b}_3$
G_2	$1/2\boldsymbol{a}_2$	G_{21}	$1/2\boldsymbol{a}_3$
		G_{22}	$1/6\boldsymbol{a}_3 + 1/3\boldsymbol{b}_3$
		G_{23}	$5/6\boldsymbol{a}_3 + 2/3\boldsymbol{b}_3$
G_3	$1/2\boldsymbol{a}_2 + 1/2\boldsymbol{b}_2$	G_{31}	$1/2\boldsymbol{a}_3 + 1/2\boldsymbol{b}_3$
		G_{32}	$1/6\boldsymbol{a}_3 + 5/6\boldsymbol{b}_3$
		G_{33}	$5/6\boldsymbol{a}_3 + 1/6\boldsymbol{b}_3$
G_4	$1/2\boldsymbol{b}_2$	G_{41}	$1/2\boldsymbol{b}_3$
		G_{42}	$2/3\boldsymbol{a}_3 + 5/6\boldsymbol{b}_3$
		G_{43}	$1/3\boldsymbol{a}_3 + 1/6\boldsymbol{b}_3$

Table 2. Matrix Element Array Generating $G_{pq}-H_r$ Pairs

ith\\(i+1)th	H_r	H_r	H_r	H_r
G_{1q}	1	0	0	0
G_{2q}	0	1	0	0
G_{3q}	0	0	1	0
G_{4q}	0	0	0	1

When the probability table includes the matrix-elemental array indicated in Table 2, it generates $G_{pq}-H_r$ pairs from G_{pq} and H_r. The $G_{pq}-H_r$ pairs can be connected to the $G_{p'q'}-H_{r'}$ pairs by the array in Table 3 for $r \neq r'$ or that in Table 4 for $r = r$. Consequently, when arrays $\mathbf{E}$, $\mathbf{O}$, $\mathbf{A}_{st}$, $\mathbf{G}_q$, ${}^t\mathbf{G}_p$, $\mathbf{H}_r$, and ${}^t\mathbf{H}_r$ are defined in eq 1 to simplify the expression, the probability table for the 2H phase can be constructed as shown in Table 5.

$$\mathbf{E} \equiv \begin{pmatrix} 1 & 0 & 0 & 0 \\ 0 & 1 & 0 & 0 \\ 0 & 0 & 1 & 0 \\ 0 & 0 & 0 & 1 \end{pmatrix}, \mathbf{O} \equiv \begin{pmatrix} 0 & 0 & 0 & 0 \\ 0 & 0 & 0 & 0 \\ 0 & 0 & 0 & 0 \\ 0 & 0 & 0 & 0 \end{pmatrix}, \mathbf{A}_{st}$$

$$\equiv \begin{pmatrix} 0 & \alpha_{st} & \alpha_{st} & \alpha_{st} \\ \alpha_{st} & 0 & \alpha_{st} & \alpha_{st} \\ \alpha_{st} & \alpha_{st} & 0 & \alpha_{st} \\ \alpha_{st} & \alpha_{st} & \alpha_{st} & 0 \end{pmatrix}, \mathbf{G}_q$$

$$\equiv (G_{1q}G_{2q}G_{3q}G_{4q}), {}^t\mathbf{G}_q \equiv \begin{pmatrix} G_{1q} \\ G_{2q} \\ G_{3q} \\ G_{4q} \end{pmatrix}, \mathbf{H}_r$$

$$\equiv (H_rH_rH_rH_r), \text{and} {}^t\mathbf{H}_r \equiv \begin{pmatrix} H_r \\ H_r \\ H_r \\ H_r \end{pmatrix} \quad (1)$$

When the structure was analyzed on the assumption that all $\mathbf{A}_{st}$ were equal to each other, or all α_{st}'s are equal to 1/9, the commensurate model did not significantly

Table 3. Matrix Element Array Connecting G_p-H_r Pairs to $G_{p'}-H_{r'}$ pairs for $r \neq r'$

$(i-1)$th − ith\ $(i+1)$th − $(i+2)$th	$G_{1q'}-H_{r'}$	$G_{2q'}-H_{r'}$	$G_{3q}-H_{r'}$	$G_{4q'}-H_{r'}$
$G_{1q}-H_r$	0	α_{st}	α_{st}	α_{st}
$G_{2q}-H_r$	α_{st}	0	α_{st}	α_{st}
$G_{3q}-H_r$	α_{st}	α_{st}	0	α_{st}
$G_{4q}-H_r$	α_{st}	α_{st}	α_{st}	0

Table 4. Matrix Element Array Connecting G_p-H_r Pairs to $G_{p'}-H_{r'}$ Pairs for $r = r'$

$(i-1)$th − i-th\ $(i+1)$th − $(i+2)$th	$G_{1q'}-H_{r''}$	$G_{2q'}-H_{r'}$	$G_{3q}-H_{r'}$	$G_{4q'}-H_{r'}$
$G_{1q}-H_r$	0	0	0	0
$G_{2q}-H_r$	0	0	0	0
$G_{3q}-H_r$	0	0	0	0
$G_{4q}-H_r$	0	0	0	0

Table 5. Probability Table for 2H Phase

	G_1	G_2	G_3	G_1	G_2	G_3	H_1	H_1	H_1	$H_{1'}$	$H_{1'}$	$H_{1'}$
$^tG_1$	**O**	**O**	**O**	**O**	**O**	**O**	**O**	**O**	**O**	**E**	**O**	**O**
$^tG_2$	**O**	**O**	**O**	**O**	**O**	**O**	**O**	**O**	**O**	**O**	**E**	**O**
$^tG_3$	**O**	**O**	**O**	**O**	**O**	**O**	**O**	**O**	**O**	**O**	**O**	**E**
$^tG_1$	**O**	**O**	**O**	**O**	**O**	**O**	**E**	**O**	**O**	**O**	**O**	**O**
$^tG_2$	**O**	**O**	**O**	**O**	**O**	**O**	**O**	**E**	**O**	**O**	**O**	**O**
$^tG_3$	**O**	**O**	**O**	**O**	**O**	**O**	**O**	**O**	E	O	**O**	**O**
$^tH_1$	$\mathbf{A_{11}}$	$\mathbf{A_{12}}$	$\mathbf{A_{13}}$	**O**	**O**	**O**	**O**	**O**	**O**	**O**	**O**	**O**
$^tH_1$	$\mathbf{A_{21}}$	$\mathbf{A_{22}}$	$\mathbf{A_{23}}$	**O**	**O**	**O**	**O**	**O**	**O**	**O**	**O**	**O**
$^tH_1$	$\mathbf{I_{31}}$	$\mathbf{A_{32}}$	$\mathbf{A_{33}}$	**O**	**O**	**O**	**O**	**O**	**O**	**O**	**O**	**O**
$^tH_{1'}$	**O**	**O**	**O**	$\mathbf{A_{44}}$	$\mathbf{A_{45}}$	$\mathbf{A_{46}}$	**O**	**O**	**O**	**O**	**O**	**O**
$^tH_{1'}$	**O**	**O**	**O**	$\mathbf{A_{54}}$	$\mathbf{A_{55}}$	$\mathbf{A_{56}}$	**O**	**O**	**O**	**O**	**O**	**O**
$^tH_{1'}$	**O**	**O**	**O**	$\mathbf{A_{64}}$	$\mathbf{A_{65}}$	$\mathbf{A_{66}}$	**O**	**O**	**O**	**O**	**O**	**O**

improve the fitting results. However, when $\mathbf{A_{s3}} = \mathbf{A_{s5}} = \mathbf{O}$, or $\alpha_{s1} = \alpha_{s2} = \alpha_{s4} = \alpha_{s6} = 1/6$ and $\alpha_{s3} = \alpha_{s5} = 0$, the R factors were lowered from $R_p = 5.75\%$ and $R_{wp} = 9.12\%$ by the incommensurate model[3] to $R_p = 4.18\%$ and $R_{wp} = 6.05\%$. It should be noted that such selection did not improve the fitting results using the incommensurate model as shown in the Supporting Information; therefore, it can be concluded that the better fitting results did not stem from the modified stacking manner of the guest layers but rather from the commensurate model.

Chemical analyses for the superconductors revealed that not only the sodium ions but also oxonium (H_3O^+) ions are charge-balancing ions in the galleries;[15] however, they were not taken into account in our previous structure analysis. In the present structure model, the D_3O^+ ions were introduced near the Na^+ sites, because the oxonium content was strongly correlated with the Na content.

When the guest compositions were changed by acid[6a] or alkaline[6b] treatment, the total content of oxonium and Na remained almost constant. The increasing oxonium content upon acid treatment decreased the Na content and vice versa upon alkaline treatment. That is, the acid treatment seems to increase the vacant Na sites, which are occupied by oxonium ions, and the alkaline treatment seems to introduce Na^+ ions along with repelling oxonium ions. Therefore, it is reasonable that oxonium and Na^+ ions would be located at the same or nearby crystallographic sites. In addition, Raman spectroscopy revealed that oxonium ions would be located near the Na sites.[15]

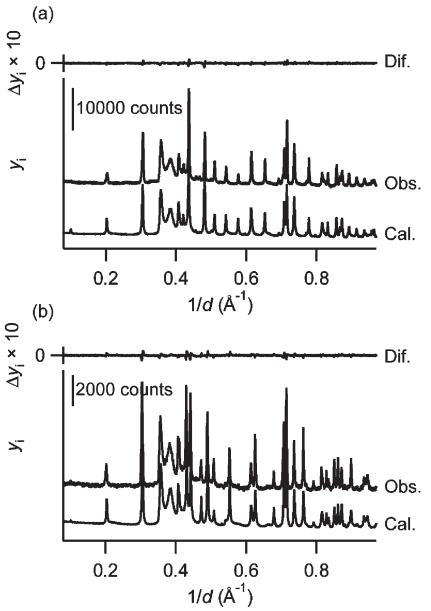

Figure 2. Pattern fitting results for (a) 2H and (b) 3R phases. In each panel, the curves indicate calculated and observed patterns and their weighted difference from bottom to top. The difference, Δy_i, was calculated by $(y_{io} - y_{ic})/\sigma_i$, where y_{io}, y_{ic}, and σ_i are the observed and calculated intensities and the statistical uncertainty of the i-th point, respectively. Differences were multiplied by 10 to make the plots easier to read.

There are two sodium sites, Na1 and Na2, which were fully and partially occupied, respectively. When the oxonium ions were introduced near the Na2 sites, the R factors further decreased to $R_p = 3.95\%$ and $R_{wp} = 5.62\%$. The observed and calculated patterns are compared in Figure 2a, and the final structure parameters are listed in Table 6.

Commensurate Model for the 3R Phase and Structure Refinement. Because the host and guest layers are almost identical between the two phases, the structure models refined for the 2H phase can be used for the 3R phase. The probability table for the 3R phase was obtained in the same procedure as mentioned above to meet the requirement of $p(G_{pq}-H_r, G_{p'q'}-H_{r'}) = 0$ for $p = p'$ or $(r, r') \neq (1, 2), (2, 3)$, or $(3, 1)$, which is indicated in Table 7. However, this is not enough for the commensurate model to reproduce the diffraction pattern for the 3R phase. The calculated intensity ratio between 104 and 015 reflections, where 104 and 105 were Miller indices based on the $a \times a \times c_{3R}$ lattice, was quite different from the observed one, as shown in Figure 3a. Another set of guest layers was introduced into the structure model to improve the fitting result.

Co in the hosts and Na in the guests are octahedrally coordinated by O and D_2O, respectively, to form trigonal lattices. When the three positions in the host trigonal lattice, (0, 0), (2/3, 1/3), and (1/3, 2/3), are denoted by A1, B1, and C1, respectively, the O−Co—O stacking sequence in the host layer can be expressed as A1(O)—B1(Co)—C1(O)—[ ]—C1(O)—A1(Co)—B1(O), where [ ]

(15) (a) Takada, K.; Fukuda, K.; Osada, M.; Nakai, I.; Izumi, F.; Dilanian, R. A.; Kato, K.; Takata, M.; Sakurai, H.; Takayama-Muromachi, E.; Sasaki, T. *J. Mater. Chem.* **2004**, *14*, 1448. (b) Takada, K.; Osada, M.; Izumi, F.; Sakurai, H.; Takayama-Muromachi, E.; Sasaki, T. *Chem. Mater.* **2005**, *17*, 2034.

Table 6. Fractional Coordinates; Occupancies, *g*; and Isotropic Atomic Displacement Parameters, *B*; for 2H phase[a]

host part	*x*	*y*	*z*	*g*	*B* (Å^2)
Co1	0	0	0	1	0.735(4)
Co2	1/2	0	0	1	= *B*(Co1)
O1	2/3	1/3	−0.2328(5)	1	= *B*(Co1)
O2	0.1672(7)	−0.1672	−0.1942(2)	1	= *B*(Co1)
guest part	*x*	*y*	*z*	*g*	*B* (Å^2)
Na1	0	0	0	1[b]	= *B*(Co1)
Na2	1/3	2/3	0.1596(12)	0.192[b]	= *B*(Co1)
O3	0.6840(6)	0.6662(8)	0.2808(6)	0.857(1)	= *B*(Co1)
D1	0.7352(6)	0.6876(11)	0.4747(5)	= *g*(O3)	5.73(3)
D2	0.4934(5)	0.5496(6)	0.2712(7)	= *g*(O3)	= *B*(D1)
O4	2/3	1/3	0.3798(10)	0.146(3)	= *B*(Co1)
D3	0.41(3)	0.299(2)	= *z*(O4)	= *g*(O4)	= *B*(D1)

[a] $a = 5.6418(2)$ Å, $c = 4.9029(3)$ Å, and $\gamma = 120°$. Local symmetry: $x, y, z; -y, x-y, z; y-x, -x, z; -x, -y, -z; y, y-x, -z; x-y, x, -z$. [b] Na content was fixed to the analytical value.

Table 7. Probability Table for 3R Phase

	G_1	G_2	G_3	G_1	G_2	G_3	G_1	G_2	G_3	H_1	H_1	H_1	H_2	H_2	I_2	H_3	H_3	H_3
$^tG_1$	O	O	O	O	O	O	O	O	O	O	O	O	E	O	O	O	O	O
$^tG_2$	O	O	O	O	O	O	O	O	O	O	O	O	O	E	O	O	O	O
$^tG_3$	O	O	O	O	O	O	O	O	O	O	O	O	O	O	E	O	O	O
$^tG_1$	O	O	O	O	O	O	O	O	O	O	O	O	O	O	O	E	O	O
$^tG_2$	O	O	O	O	O	O	O	O	O	O	O	O	O	O	O	O	E	O
$^tG_3$	O	O	O	O	O	O	O	O	O	O	O	O	O	O	O	O	O	E
$^tG_1$	O	O	O	O	O	O	O	O	O	E	O	O	O	O	O	O	O	O
$^tG_2$	O	O	O	O	O	O	O	O	O	O	E	O	O	O	O	O	O	O
$^tG_3$	O	O	O	O	O	O	O	O	O	O	O	E	O	O	O	O	O	O
$^tH_1$	A_{11}	A_{12}	A_{13}	O	O	O	O	O	O	O	O	O	O	O	O	O	O	O
$^tH_1$	A_{21}	A_{22}	A_{23}	O	O	O	O	O	O	O	O	O	O	O	O	O	O	O
$^tH_1$	A_{31}	A_{32}	A_{33}	O	O	O	O	O	O	O	O	O	O	O	O	O	O	O
$^tH_2$	O	O	O	A_{44}	A_{45}	A_{46}	O	O	O	O	O	O	O	O	O	O	O	O
$^tH_2$	O	O	O	A_{54}	A_{55}	A_{56}	O	O	O	O	O	O	O	O	O	O	O	O
$^tH_2$	O	O	O	A_{64}	A_{65}	A_{66}	O	O	O	O	O	O	O	O	O	O	O	O
$^tH_3$	O	O	O	O	O	O	A_{77}	A_{78}	A_{79}	O	O	O	O	O	O	O	O	O
$^tH_3$	O	O	O	O	O	O	A_{87}	A_{88}	A_{89}	O	O	O	O	O	O	O	O	O
$^tH_3$	O	O	O	O	O	O	A_{97}	A_{98}	A_{99}	O	O	O	O	O	O	O	O	O

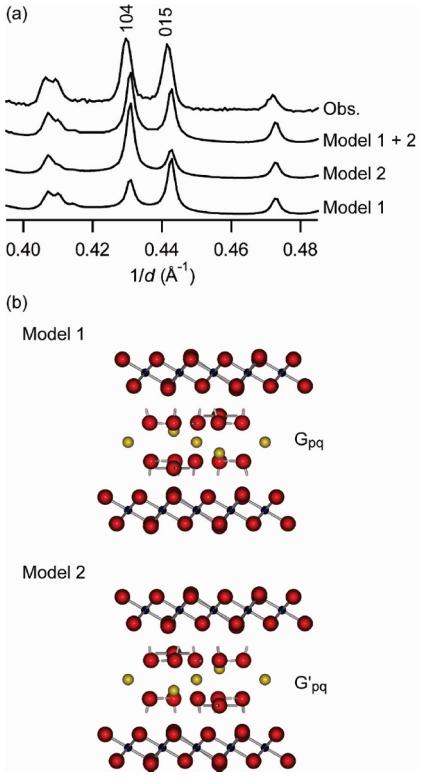

Figure 3. Observed and calculated ND patterns for 3R phases. Patterns were calculated from model 1, model 2, and a mixture of models 1 and 2.

denotes the gallery. On the other hand, when the three corresponding positions in the guest lattice are denoted by A2, B2, and C2, stacking of $D_2O-Na—D_2O$ can be also represented by A2(D_2O)—B2(Na)—C2(D_2O). Consequently, the stacking sequence in the structure model is, for example, A1(O)—B1(Co)—C1(O)—A2(D_2O)—B2(Na)—C2(D_2O)—C1(O)—A1(Co)—B1(O), shown as model 1 in Figure 3b. However, sequence of A1(O)—B1(Co)—C1(O)—C2(D_2O)—B2(Na)—A2(D_2O)—C1(O)—A1(Co)—B1(O) shown as Model 2 is also possible. When the diffraction pattern from the structure model was calculated using G'_{pq} generated from G_{pq} by a symmetry operation of $(x, y, -z)$ in place of G_{pq}, the intensity ratio between the reflections became inverse. If the two kinds of the stacking are almost the same in formation energy, the sample will contain grains with both kinds of stacking with the same probability. When the two diffraction patterns were summed up on this assumption, the simulated pattern became very similar to the observed one. When $\mathbf{A}_{s3}$, $\mathbf{A}_{s4}$, and $\mathbf{A}_{s8}$ were assumed to be **O** as in the commensurate model for the 3R phase, the resultant *R* factors were $R_p = 4.11\%$ and $R_{wp} = 5.83\%$, which were significantly lower than $R_p = 5.05\%$ and $R_{wp} = 8.14\%$ obtained from the incommensurate model in our previous study. The pattern fitting results and refined structure parameters are indicated in Figure 2b and Table 8, respectively.

Table 8. Fractional Coordinates; Occupancies, *g*; and Isotropic Atomic Displacement Parameters, *B*; for 3R Phase[a]

host part	*x*	*y*	*z*	*g*	*B* (Å^2)
Co1	0	0	0	1	0.553(5)
Co2	1/2	0	0	1	= *B*(Co1)
O1	2/3	1/3	−0.2288(6)	1	= *B*(Co1)
O2	0.1675(10)	−0.1675	−0.1900(3)	1	= *B*(Co1)
guest part	*x*	*y*	*z*	*g*	*B* (Å^2)
Na1	0	0	0	1[b]	= *B*(Co1)
Na2	1/3	2/3	0.153(3)	0.206[b]	= *B*(Co1)
O3	0.6972(7)	0.6772(10)	0.2859(6)	0.836(1)	= *B*(Co1)
D1	0.7519(5)	0.6789(10)	0.4715(8)	= *g*(O3)	4.15(2)
D2	0.5046(8)	0.5499(7)	0.2773(5)	= *g*(O3)	= *B*(D1)
O4	2/3	1/3	0.394(3)	0.153(2)	= *B*(Co1)
D3	0.4369(13)	0.272(2)	= *z*(O4)	= *g*(O4)	= *B*(D1)

[a] $a = 5.6483(4)$ Å, $c = 4.9127(7)$ Å, and $\gamma = 120°$. Local symmetry: $x, y, z; -y, x-y, z; y-x, -x, z; -x, -y, -z; y, y-x, -z; x-y, x, -z$. [b] Na content was fixed to the analytical value.

Table 9. Co−O Bond Lengths in CoO_6 Octahedra and Bond Valence Sums (BVS)

	2H		3R	
	Co−O (Å)	BVS	Co−O (Å)	BVS
Co1−O2 (× 6)	1.891(3)	3.58	1.886(3)	3.63
Co2−O1 (× 2)	1.989(1)	3.35	1.980(2)	3.43
Co2−O2 (× 4)	1.884(2)		1.875(4)	
average	1.905(2)	3.41	1.898(3)	3.48
Co oxidation states determined by chemical analyses	+3.40 to +3.41,[6a] +3.48,[6b] +3.42 to +3.43,[15a] +3.46[17a]		+3.48,[1b] +3.47 to +3.52[17b]	

It is not necessary to take into account such a situation for the 2H phase, because the 2H host subsystem has a mirror plane in the middle of the galleries. The two sets of guest layers result in the stacking sequences of A1(O)—B1(Co)—C1(O)—A2(D_2O)—B2(Na)—C2(D_2O)—C1(O)—B1(Co)—A1(O) and A1(O)—B1(Co)—C1(O)—C2(D_2O)—B2(Na)—A2(D_2O)—C1(O)—B1(Co)—A1(O) and should not make any difference in the diffraction pattern.

Another possible structure model had been already checked. In the above structure models, the host lattice was stacked right above the guest lattice. For example, H_1 was stacked right above G_{11}, sharing a 3-fold axis. However, the stacking may be accompanied by a lateral shift. When $\boldsymbol{s}_L$ corresponding to the lateral shift was introduced in the structure model in order to check this possibility, $\boldsymbol{s}_L$ was converged to $\boldsymbol{0}$ in the refinement.

Discussion

Revisit to the Incommensurate Model. It is better to revisit the incommensurate structure model before concluding that the host and guest layers are commensurate with each other, because the incommensurate and commensurate models are different in the host and guest structures as well as in the degree of the commensuration. The host has an $a \times a$ trigonal lattice in the incommensurate model, whereas it is $2a \times 2a$ in the commensurate one. On the other hand, two kinds of guest layers were used in the incommensurate model, one of which has a $2/\sqrt{3}a \times 2/\sqrt{3}a$ lattice, and the other has $2a \times 2a$. Even when the $2a \times 2a$ guest layer was used, the guest layer did not include H_3O ions that were introduced in the present commensurate model. Therefore, it should be made clear that the improvement in the fitting result comes not from the different host and guest structures but from their commensurate relation before further discussion.

The simplest way to reach the conclusion is to simulate the diffraction patterns from an incommensurate model with the same host and guest structures as those refined on the basis of the present commensurate model and compare the fitting results. As shown in the Supporting Information, the fitting results from the incommensurate models were significantly worse than those from the commensurate models. Therefore, it can be concluded that the improvement of the fitting results in this study originated from their commensurate relation between the host and guest layers.

Co−O Bond Length and Co Oxidation State. The above structural analysis based on the commensurate structure models gave lower *R* factors than that on the incommensurate models, which suggests that the CoO_2 layer has a 2×2 superstructure. This may modulate, for example, electron distribution in the CoO_2 layers. Therefore, it is worth discussing the Co−O bond length, because Co valence state corresponding to electron distribution can be estimated from the bond length by bond valence calculation.[16]

In addition, the Co−O bonds reported in literature were abnormally short. The valence states of Co were determined to be between +3.4 and +3.5 by redox titration.[1b,6,15a,17] Although the bond length is expected to be 1.90 Å from the valence state by bond-valence calculation with bond valence parameter of 1.70 for Co,[18] the refined lengths from the XRD[1b,15a] and ND[2] data were only around 1.87 Å; its corresponding oxidation state is +3.8. Such short bond

(16) Brown, I. D.; Altermatt, D. *Acta Crystallogr., Sect. B* **1985**, *41*, 244.
(17) (a) Karppinen, M.; Asako, I.; Motohashi, T.; Yamauchi, H. *Chem. Mater.* **2004**, *16*, 1693. (b) Sakurai, H.; Takada, K.; Sasaki, T.; Izumi, F.; Dilanian, R. A.; Takayama-Muromachi, E. *J. Phys. Soc. Jpn.* **2004**, *73*, 2590.
(18) Brese, N. E.; O'Keeffe, M. *Acta Crystallogr., Sect. B* **1991**, *47*, 192.

lengths may come from the inaccurate guest arrangement. Because H_2O or D_2O molecules reside very close to the O atoms in the CoO_2 layers, their positions are strongly correlated to each other in the refinement; that is, inaccurate D_2O position tends to result in the incorrect O position and Co−O distance.

Table 10. Sets of D1−O (host) Distances (*l*'s) and O3−D1−O (host) angles (ϕ's) Found between Host and Guest Layers in 2H Phase

	l (Å)	ϕ (deg)
set 1	1.563	166.3
	1.739	168.2
	1.736	168.3
set 2	1.789	135.5
	1.947	138.5
	1.942	138.7
set 3	1.880	125.9
	2.030	129.3
	2.025	129.5
set 4	1.738 × 3	168.1 × 3
set 5	1.945 × 3	138.5 × 3
set 6	2.028 × 3	129.3 × 3

Table 11. *i*th Host − (*i*+1)th Guest − (*i*+2)th Host Sequences and Sets of *l*'s and ϕ's between the *i*th Host and (*i*+1)th Guest and between the (*i*+1)th Guest and (*i*+2)th Host in 2H Phase, Where $p = 2$, 3, and 4

*i*th host − (*i*+1)th guest − (*i*+2)th host	*l* and ϕ between *i*th host and (*i*+1)th guest	*l* and ϕ between (*i*+1)th guest and (*i*+2)th host
$H_1-G_{p2}-H_{1'}, H_{1'}-G_{p1}-H_1$	set 1	set 2
$H_1-G_{p1}-H_{1'}, H_{1'}-G_{p3}-H_1$	set 2	set 1
$H_1-G_{p3}-H_{1'}, H_{1'}-G_{p2}-H_1$	set 3	set 3
$H_1-G_{12}-H_{1'}, H_{1'}-G_{11}-H_1$	set 4	set 5
$H_1-G_{11}-H_{1'}, H_{1'}-G_{13}-H_1$	set 5	set 4
$H_1-G_{13}-H_{1'}, H_{1'}-G_{12}-H_1$	set 6	set 6

Table 12. Sets of D1−O (host) Distances (*l*'s) and O3−D1−O (host) Angles (ϕ's) found between Host and Guest Layers in 3R Phase

	l (Å)	ϕ (deg)
set 1	1.571	177.3
	1.734	177.2
	1.730	176.9
set 2	1.906	126.3
	2.045	129.0
	2.038	129.3
set 3	1.957	124.8
	2.091	127.6
	2.083	127.8
set 4	1.732 × 3	177.1 × 3
set 5	2.044 × 3	129.1 × 3
set 6	2.088 × 3	127.8 × 3

Table 9 lists the Co−O bond lengths in the CoO_2 layers and the bond valence sums corresponding to the valence states of Co calculated from the bond lengths. The bond lengths ranged from 1.87 to 1.99 Å with an average of 1.90 Å, and the averaged bond valence sums were +3.41 and +3.48 for the 2H and 3R phases, respectively. The bonds were longer than those were reported, and the bond valence sums well agreed with the Co oxidation states determined by chemical analyses.

Stacking Manner of the Guest Layers. The "short-range interlayer ordering" allows nine kinds of guest layers as the (*i*+1)th to be stacked on the *i*th layer. However, six kinds were selected from the nine in the above analyses to improve the fitting results. Although it has not been clarified why the other three are forbidden, one conceivable explanation is given below.

Because such selection did not improve the refinement results based on the incommensurate models, the improvement would be connected to the relative position between the host and guest layers, which does not appear in the diffraction patterns simulated by the incommensurate model.

The relative position will be dominated by the interaction between D1 in D_2O and adjoining O in the host, because positively charged D1 will attract negatively charged O (host). The attraction will make the D1−O distance and the O3−D1−O (host) connection as short and close to 180° as possible, respectively, to stabilize the structure. To determine which guest layer in which gallery stabilizes the structure, the interatomic distance (*l*) and the bond angle (ϕ) were calculated for every host−guest combination.

The calculated (l, ϕ)'s for the 2H phase are listed in Tables 10 and 11. For instance, when G_{22} is interposed as the (*i*+1)th layer between the *i*th H_1 and the (*i*+2)th $H_{1'}$, the three D_2O molecules facing the H1 are bonded to O (host) with (l, ϕ) = (1.789 Å, 135.5°), (1.947 Å, 138.5°), (1.942 Å, 138.7°), and those facing the H1′ are with (l, ϕ) = (1.563 Å, 166.3°), (1.739 Å, 168.2°), and (1.736 Å. 168.3°). On the other hand, when G_{13} is interposed between H_1 and $H_{1'}$, all the D_2O molecules in G_{13} are bonded to the host layers with l = 2.028 Å and ϕ = 129.3°. Because the interpositions forming (l, ϕ)'s in sets 3 and 6 are less preferential, sequences of $H_1-G_{p3}-H_1'$, $H_{1'}-G_{p2}-H_1$ with p = 1−4 will be forbidden. The matrix arrays to result in the sequences in

Table 13. *i*th Host − (*i*+1)th Guest − (*i*+2)th host sequences and sets of *l*'s and ϕ's between the *i*th host and (*i*+1)th guest and between the (*i*+1)th guest and (*i*+2)th Host in 3R Phase, Where $p = 2$, 3, and 4

*i*th host − (*i*+1)th guest − (*i*+2)th host	*l* and ϕ between *i*th host and (*i*+1)th guest	*l* and ϕ between (*i*+1)th guest and (*i*+2)th host
$H_1-G_{p2}-H_2, H_2-G_{p3}-H_3, H_3-G_{p1}-H_1,$ $H_1-G'_{p1}-H_2, H_2-G'_{p2}-H_3, H_3-G'_{p3}-H_1$	set 1	set 2
$H_1-Gp_1-H_2, H_2-G_{p2}-H_3, H_3-G_{p3}-H_1,$ $H_1-G'_{p2}-H_2, H_2-G'_{p3}-H_3, H_3-G'_{p1}-H_1$	set 2	set 1
$H_1-G_{p3}-H_2, H_2-G_{p1}-H_3, H_3-G_{p2}-H_1,$ $H_1-G'_{p3}-H_2, H_2-G'_{p1}-H_3, H_3-G'_{p2}-H_1$	set 3	set 3
$H_1-G_{12}-H_2, H_2-Q_{13}-H_3, H_3-G_{11}-H_1,$ $H_1-G'_{11}-H_2, H_2-G'_{12}-H_3, H_3-G'_{13}-H_1$	set 4	set 5
$H_1-G_{11}-H_2, H_2-G_{12}-H_3, H_3-G_{13}-H_1,$ $H_1-G'_{12}-H_2, H_2-G'_{13}-H_3, H_3-G'_{11}-H_1$	set 5	set 4
$H_1-G_{13}-H_2, H_2-G_{11}-H_3, H_3-G_{12}-H_1,$ $H_1-G'_{13}-H_2, H_2-G'_{11}-H_3, H_3-G'_{12}-H_3$	set 6	set 6

Table 5 are $\mathbf{A}_{s3}$ and $\mathbf{A}_{s5}$, which were set at **O** in the above refinement. Similarly, for the 3R phase, the arrays that were set at **O** in the refinement generate the less preferential sequences, where sets 3 and 6 are found, as indicated in Tables 12 and 13.

Conclusions

Structure analysis for cobalt oxide superconductors based on commensurate composite crystal models revealed a 2×2 superstructure in the host and guest layers. The Co−O bond lengths calculated from the refined structure were ca. 1.90 Å, which agreed well with that expected from the Co oxidation states.

Acknowledgment. The authors acknowledge Dr. Katsuo Kato for his computer programs. This work was partially supported by World Premier International Center Initiative (WPI) on Materials Nanoarchitectonics, MEXT, Japan and CREST of the Japan and Technology Agency (JST).

Supporting Information Available: Additional information (PDF). This material is available free of charge via the Internet at http://pubs.acs.org.